0026-895X/05/6701-69–77$20.00
MOLECULAR PHARMACOLOGY
Copyright © 2005 The American Society for Pharmacology and Experimental Therapeutics
Mol Pharmacol 67:69–77, 2005

Vol. 67, No. 1
5553/1189060
Printed in U.S.A.

Ertiprotafib Improves Glycemic Control and Lowers Lipids via Multiple Mechanisms

David V. Erbe, Suyue Wang, Yan-Ling Zhang, Kimberly Harding, Leslie Kung, May Tam, Leslie Stolz, Yuzhe Xing, Sarah Furey, Ariful Qadri, Lori D. Klaman, and James F. Tobin

Wyeth Research, Cardiovascular and Metabolic Diseases, Cambridge, Massachusetts

Received July 28, 2004; accepted October 7, 2004

ABSTRACT

Ertiprotafib belongs to a novel class of insulin sensitizers developed for treatment of type 2 diabetes. In insulin-resistant rodent models, ertiprotafib and a close analog lowered both fasting blood glucose and insulin levels and improved glycemic excursion during an oral glucose tolerance test. In addition, treatment of rodents improved lipid profiles, with significantly lowered triglyceride and free fatty acid levels. These results suggested that this therapeutic activity might involve mechanisms in addition to PTP1b inhibition. In this study, we demonstrate that ertiprotafib activates peroxisome proliferator-activated receptor (PPAR)α and PPARγ at concentrations comparable with those of known agonists of these regulators. Furthermore, it is able to drive adipocyte differentiation of C3H10T$_{1/2}$ cells, a hallmark of PPARγ activation. Livers from ertiprotafib-treated animals showed significant induction of acyl-CoA oxidase activity, probably caused by PPARα engagement in these animals. We also show that ertiprotafib inhibits PTP1b in vitro with nonclassic kinetics at concentrations above its EC$_{50}$ for PPAR agonism. Thus, the complete mechanism of action for ertiprotafib and related compounds in vivo may involve multiple independent mechanisms, including (but not necessarily limited to) PTP1b inhibition and dual PPARα/PPARγ agonism. Ertiprotafib pharmacology and interpretation of clinical results must be seen in light of this complexity.

Increasing prevalence of obesity and type 2 diabetes continues to drive the search for better pharmacologic treatments for dyslipidemia and hyperglycemia (Inzucchi, 2002; Flier, 2004). Thiazolidinediones provide a first opportunity to improve the underlying insulin resistance in patients through activation of the peroxisome proliferator-activated receptor (PPAR)-γ (PPARγ) (Willson et al., 2000; Rosen and Spiegelman, 2001). These agents regulate gene transcription in insulin-sensitive tissues, resulting ultimately in reduced glucose levels in patients through increased utilization in skeletal muscle and decreased de novo synthesis in the liver (Way et al., 2001; Willson et al., 2001). Improvements to thiazolidinedione therapy now focus on improving glycemic and lipid control while avoiding the weight gain and edema seen with these agents (Inzucchi, 2002; Diamant and Heine, 2003; Nesto et al., 2003).

One approach receiving considerable attention is to combine PPARγ agonism with activation of PPARα to create a dual agonist (Murakami et al., 1998; Brooks et al., 2001; Cronet et al., 2001; Liu et al., 2001; Lohray et al., 2001). Members of the fibrate class of lipid-lowering drugs act as agonists of PPARα to regulate fatty acid metabolism and ketogenesis in the liver (Willson et al., 2000; Kersten et al., 2000). These potent hypolipidemic agents are used to lower plasma triglyceride levels and raise high-density lipoprotein (HDL) levels. Thus, combining agonism for these receptors in a dual PPARα/γ ligand could provide clear advantages to treat the hyperglycemia and dyslipidemia in diabetic patients that have an increased risk for cardiovascular disease (Brooks et al., 2001).

Targeting the protein tyrosine phosphatase PTP1b also provides an opportunity to improve insulin sensitivity without the weight gain seen with current PPARγ activators. Genetically deficient PTP1b knockout mice remain healthy with sustained phosphorylation of the insulin receptor, which results in profound insulin sensitivity with improved glucose tolerance, and lower levels of circulating insulin (Elchebly et al., 1999; Klaman et al., 2000). Moreover, these mice have lower adiposity and are resistant to weight gain because of their increased sensitivity to leptin (Cheng et al., 2002; Zabolotny et al., 2002). In addition, mice treated with PTP1b antisense oligonucleotides show increased insulin-

Article, publication date, and citation information can be found at http://molpharm.aspetjournals.org.
doi:10.1124/mol.104.005553.

ABBREVIATIONS: PPAR, peroxisome proliferator-activated receptor; PTP1b, protein tyrosine phosphatase 1b; pNPP, *p*-nitrophenyl phosphate; SV40, simian virus 40; DME, Dulbecco's modified Eagle's; FBS, fetal bovine serum; DMSO, dimethyl sulfoxide; PPRE, peroxisome proliferator-activated receptor response element.

dependent signaling, resulting in blood glucose normalization and improved insulin sensitivity (Zinker et al., 2002; Gum et al., 2003). Thus, inhibition of PTP1b could prolong insulin receptor phosphorylation, improve insulin action, normalize glucose levels, and reduce adiposity in diabetic patients.

Members of a class of novel arylbenzonaphthothiophenes and arylbenzonaphthofurans have been developed as PTP1b inhibitors and were shown to improve insulin sensitivity in rodents (Wrobel et al., 1999). One compound from these efforts, ertiprotafib, progressed to phase II clinical trials for treatment of type 2 diabetes. However, data from in vivo treatment of rodents with ertiprotafib were inconsistent with PTP1b inhibition as the sole mechanism for these changes. It is noteworthy that bone marrow hypocellularity caused by adipocyte deposition was observed in rats treated with supratherapeutic doses of ertiprotafib, an indication of possible PPARγ activation. Furthermore, treated rats showed moderate dose-related increases in liver weights along with ultrastructural signs of peroxisome proliferation, implying potential PPARα activation (Peterson et al., 2004; Z. Tong and J. Scatina, unpublished observations; L. Casciotti and R. Peterson, unpublished observations). These observations prompted the current investigations into the mechanism of action of ertiprotafib.

In this study, we show that ertiprotafib robustly increases insulin sensitivity in both mouse and rat models of insulin resistance. In addition to effects on hyperglycemia and hyperinsulinemia, ertiprotafib and a close analog also dramatically reduce both serum triglyceride and free fatty acid levels in these insulin-resistant rodent models. In vitro assays indicated the likelihood that multiple independent pathways might contribute to the full pharmacological profile of ertiprotafib. It is noteworthy that ertiprotafib was shown to inhibit PTP1b in a time-dependent, enzyme concentration-dependent manner not associated with classic competitive inhibition. In addition, PTP inhibition in cells occurred at relatively high (above 10 μM) concentrations. Further cellular studies indicated that ertiprotafib is at least a dual PPARα and PPARγ agonist, with EC_{50} values for transactivation near 1 μM, and is able to induce adipocyte differentiation of fibroblast cells, probably through PPARγ. Finally, livers from animals treated with ertiprotafib showed significant induction of the PPARα-dependent enzyme, acyl-CoA oxidase. Taken together, these data indicate that ertiprotafib seems to use a complicated mechanism of action in vivo, involving at least engagement of PPARα and -γ, in addition to possible PTP1b inhibition, to improve insulin sensitivity and lower lipids.

Materials and Methods

PTP1b Assays. Cell-free assays used recombinant human PTP1b (residues 1–299 expressed and purified from *Escherichia coli*) in 96-well plates containing 200 μl of dimethyl glutaric acid buffer (50 mM 3,3-dimethyl glutaric acid, ionic strength = 0.15 M, 0.01% Triton X-100, 1 mM EDTA, and 1 mM Tris(2-carboxyethyl)phosphine hydrochloride, pH 7.0) plus 1 mM *p*-nitrophenyl phosphate substrate and various concentrations of inhibitors. Reactions were initiated by the addition of enzyme. Measuring liberation of *p*-nitro phenyl at OD_{405} monitored reaction progress, with IC_{50} values calculated based on initial rates. Experiments determining time dependence, enzyme concentration dependence, and effects of detergents on inhibition were as described in the figure legends. Cellular assays of PTP1b activity were as described previously (Cromlish et al., 1999) with minor modifications. In brief, PTP1b was cloned into the baculovirus transfer vector pBlueBac4.5 (Invitrogen, Carlsbad, CA), and high titer recombinant viral stocks (4.7×10^8 plaque-forming unit/ml) were generated by the manufacturer (Invitrogen) to infect sf21 cells (Invitrogen) at a multiplicity of infection of 10. Infected cells were harvested by washing and centrifugation using Hanks' balanced salt solution buffered with 15 mM HEPES, pH 7.4. PTP1b activity was then measured in 200 μl of Hanks' balanced salt solution containing 5×10^4 cells premixed with inhibitors at various concentrations for 30 min, followed by addition of 1 mM pNPP (final concentration) to initiate the reaction. Reaction progress was monitored after 15 min by measuring OD_{405}.

Plasmid Construction. PPARα and PPARγ were cloned from Human Placenta Quick-Clone cDNA (BD Biosciences Clontech, Palo, Alto, CA). PPARγ was cloned by nested polymerase chain reaction, first with the primers 5′-CGAGGACACCGGAGAGGGGCGCCAC-3′ and 5′-GGGAAATGTTGGCAGTGGCTCAGG-3′, followed by the set 5′-TCCGTCGACAAGTCTAGAACCACCATGACCATGGTTGACAC-AGAG-3′ and 5′-GTGGTGGTGGCCCGGGCTAGTACAAGTC-CTTGTA-3′ to allow insertion into the XbaI/SmaI site of the plasmid pED (Kaufman et al., 1991). PPARα was cloned by polymerase chain reaction into pCR4-TOPO (Invitrogen) using the single set of primers 5′-TACTAGTACCACCATGGTGGACACGGAAAGCCCAC-3′ and 5′-TACTAGTTCAGTACATGTCCCTGTAGATCTCCT-3′, followed by digestion with SpeI and insertion into the XbaI site of pED. The PPAR response element reporter construct (pGL-3.PPRE) was made using the vector pGL3-promoter (Promega, Madison, WI) to allow for regulated expression of luciferase in a background with the SV40 promoter as described by the manufacturer. Three copies of the common PPAR response element (Willson et al., 2000) were inserted as direct repeats using the following dephosphorylated primers annealed together: 5′-CAGGGGACCAGGACAAAGGTCACGT-TCGGGAAGGGGACCAGGACAAGG TCAC GTTCGGGAAGGG-GACCAGGACAAAGGTCACGTTCGGGAC-3′ and 5′-TCGAGT-CCCGAACGTGACCTTTGTCCTGGTCCCCTTCCCGAACGTGAC-CTTTGTCCTGGTCCCCTTCCCGAACGTGACCTTTGTCCTGGTC-CCCTGGTAC-3′. The annealed oligomers were then cut and ligated into the KpnI and XhoI sites of pGL3-promoter, placing this regulatory sequence 16 bp upstream of the SV40 promoter and 248 bp upstream of the luciferase coding sequence.

Transcriptional Activation Assays. CV-1 cells (American Type Culture Collection, Manassas, VA) were plated in 12-well plates 1 day before transfection, grown to 60 to 80% confluence, and cotransfected with either pED.PPARγ, pED.PPARα, or pED alone along with pGL-3-PPRE (0.1 μg of DNA each) using LipofectAMINE (Invitrogen) according to the manufacturer. Six hours after changing to normal growth medium (DME with 10% FBS), compounds were added and cells were incubated for 40 h, harvested, and assayed for luciferase activity using the Luciferase Assay System (Promega) per the manufacturer's instructions.

Adipocyte Differentiation. C3H10T1/2 Clone 8 cells (American Type Culture Collection) were grown in 100 × 20-mm treated polystyrene cell culture dishes (Corning, Palo Alto, CA) in DME medium with 10% FBS. One day after confluence, cells were treated with compounds in the presence of 200 nM insulin for 2 days. Fresh media and test compounds were added (without insulin) for another 3 days. Accumulation of lipid droplets in cells was determined by staining with the lipophilic dye, Oil Red O (Aldrich Chemical Co., Milwaukee, WI), by washing once with PBS, fixing with 10% formalin for 10 min, washing once with PBS and once with 60% 2-proponal, and incubating with 0.3% Oil Red O in 60% 2-propanol for 15 min. Cells were then quickly washed once with 60% 2-proponal and once with water before visualization and photography.

3T3-L1 Differentiation. 3T3-L1 preadipocytes (American Type Culture Collection) were seeded at a density of 2×10^4 cells/ml (2×10^5 cells/dish) and grown to confluence in DME supplemented with

10% calf serum in 100 × 20-mm treated polystyrene cell culture dishes (Corning). Two days after confluence, media was changed to DME plus 10% FBS, 0.5 mM 3-isobutyl-1-methylxanthine, 0.25 μM dexamethasone, and 1 μg/ml insulin for 2 days followed by incubation in DME 10% FBS plus 1 μg/ml insulin for another 2 days. Finally, cells were incubated in DME with 10% FBS only (no insulin) with fresh media every 2 days until more than 90% were differentiated. Cells were then incubated in serum-free DME overnight before assay.

Phosphorylation Assay. After overnight incubation in serum free medium, 3T3-L1 adipocytes were treated with 10 μM ertiprotafib or 10 μM vanadate for 30 min, plus 10 nM insulin for an additional 10 min. Cells were washed three times to remove the insulin, and serum free media with compounds were added back for an additional hour to allow for dephosphorylation of the insulin receptor and IRS-1. Cells were then harvested in radioimmunoprecipitation assay buffer with protease inhibitors and 1 mM vanadate, vortexed, and centrifuged. Supernatants were blotted directly with HRP-conjugated anti-phosphotyrosine clone 4G10 (Upstate Biotechnology, Lake Placid, NY), followed by detection with ECL (Amersham Biosciences, Piscataway, NJ).

Glucose Uptake. Differentiated 3T3-L1 adipocytes were incubated in serum-free DME for 2 h, washed with KPH buffer (136 mM NaCl, 4.7 mM KCl, 1.25 mM $CaCl_2$, 1.25 mM $MgSO_4$, and 10 mM HEPES, pH 7.4) and pretreated with DMSO or ertiprotafib in KPH buffer for 30 min. Insulin (100 nM) (or buffer) was then added for 15 min before addition of 2-deoxy-D-[2,6-^{3}H]glucose (Pfizer, New York, NY) at 5 μM (1 μCi/ml) for various times. Glucose transport was stopped by three rapid washes in ice-cold PBS. Cells were solubilized in 0.1% SDS, and incorporated radioactivity was quantified by liquid scintillation.

Animals. Male *Ob/ob* mice were purchased from The Jackson Laboratory (Bar Harbor, ME) and were acclimated upon arrival before study. They were kept on a 12-h/12-h light/dark cycle and fed Rodent Diet 5001 (for mice and rats) from Purina Mills (Pharma Serv, Framingham, MA). Male Zucker *fa/fa* rats were purchased from Charles River Laboratories, Inc. (Wilmington, MA) and were also acclimated to a 12-h/12-h light/dark and fed the Rodent Diet 5001. Compounds were dosed orally by gavage in an aqueous suspension of 2% Tween 80 and 0.5% methylcellulose. All experimental work was conducted in accordance with the humane guidelines for ethical and sensitive care of the Institutional Animal Care and Use Committee of the United States National Institutes of Health.

Glucose, Insulin, and Lipid Measurements. Whole blood (5 μl) was used for glucose readings via tail nick for measurement using the Ascensia Elite XL glucometer and glucose strips (Bayer Corporation, Elkart, IN) by preloading a strip into the meter and touching the end to a small drop of blood on each tail as instructed by the manufacturer. For insulin measurements, blood was collected by cardiac puncture, centrifuged at 8000 rpm for 10 min, and the serum was collected and stored at −80°C until used. Insulin levels were quantified by enzyme-linked immunosorbent assay using the ultra sensitive rat insulin enzyme-linked immunosorbent assay kit from Crystal Chem. Inc. (Downers Grove, IL) per the manufacturer's instructions. In brief, anti-insulin antibody coated microplates were incubated with 100 μl/well of samples and standards at various concentrations in the sample diluent provided for 2 h at 4°C. Wells were then aspirated, washed five times with 300 μl of washing buffer (provided), and blotted dry. 100 μl of insulin enzyme conjugate was then added to each well, followed by room temperature incubation for 30 min, aspiration, seven washes, and blotting before addition of 100 μl/well of enzyme substrate solution. After 40 min at room temperature, reactions were stopped with 100 μl/well enzyme reaction stopping solution and absorbance was measured at 450 nm. After subtracting absorbance at 630 nm, insulin concentrations were calculated from the standard curves established in each experiment. Serum triglyceride levels were determined using a kit from Sigma (St. Louis, MO) according to the manufacturer's instructions by mixing 10 μl of water, glycerol standards, or samples into 0.8 ml of the free glycerol reagent (prepared according to the manufacturer's instructions) followed by incubation for 15 min at room temperature and reading the initial absorbance at 540 nm. The triglyceride reagent (0.2 ml) was then added in each cuvette, followed by mixing and incubation for an additional 15 min at room temperature. After recording each final absorbance at 540 nm, triglyceride levels were calculated (subtracting water blanks) as instructed. Serum free fatty acid levels were determined by colorimetry using the free fatty acids kit from Wako Chemicals (Richmond, VA). This method measures the nonesterified fatty acids present using acyl-CoA synthetase to produce acyl-CoA, which is then oxidized by added acyl-CoA oxidase, producing hydrogen peroxide. In the presence of peroxidase, the generated hydrogen peroxide condenses 3-methyl-*N*-ethyl-*N*-(β-hydroxyethyl)-aniline (MEHA) with 4-aminoantipyrine, and the resultant color is measured spectrophotometrically at 550 nm. Sample preparation, assays, and calculations for free fatty acid levels were performed as instructed by the manufacturer.

Oral Glucose Tolerance Test. Food was removed at least 12 h before evaluation of glucose disposal. After a tail vein glucose measurement, animals were allowed to recover before receiving an oral bolus of glucose (2 g/kg). Time points were then collected as indicated using tail vein bleeds for glucose levels as above.

Palmitoyl-CoA Oxidase Assay. Liver samples were excised from rats, snap frozen in liquid nitrogen, and stored at −80°C until processed. Liver microsomes were prepared first by homogenization in a Teflon-glass Potter S mechanical homogenizer with a 5× volume of 50 mM Tris-HCl, pH 7.4, with 0.25 M sucrose, 154 mM potassium chloride, and 1 mM EDTA. Microsomes were then purified by differential ultracentrifugation (Aitio and Vainio, 1976), and the protein content of each microsomal fraction was determined with the Bio-Rad (Hercules, CA) protein assay. Palmitoyl-CoA oxidation was measured with modifications of a method described previously (Gray et al., 1983). In brief, cuvettes contained 50 μM palmitoyl-CoA, 0.25 mM NAD^+, 0.1 mM coenzyme A, 5 mM dithiothreitol, 1.5 mM KCN, 10 μM FAD, 0.01% (w/v) Triton X-100, 0.15 mg of bovine serum albumin, and 0.8 mg of liver homogenate in 1 ml of 50 mM Tris-HCl buffer, pH 7.6. Reference cuvettes had no palmitoyl-CoA. The reaction was monitored every 30 s for 30 min at 340 nm at 37°C in a

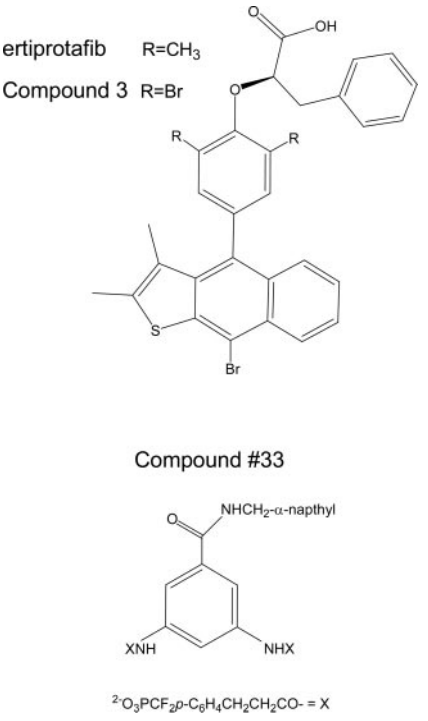

Fig. 1. Structures of ertiprotafib and compound 3.

Hitachi U-3010 Spectrophotometer. Activity was quantified as nanomoles of NADH formed per minute per milligram of homogenate protein using 6.22 cm^{-1} mM^{-1} as an extinction coefficient. All reagents were purchased from Sigma.

Results

Ertiprotafib and a close analog, compound 3 (see Fig. 1 for structures), were originally developed as in vitro inhibitors of PTP1b capable of improving insulin sensitivity in mice. Table 1 shows an example of the results after 4 days of treatment with ertiprotafib in the leptin-deficient *ob/ob* mouse model. Here, 11-week-old male *ob/ob* mice were placed into two similar groups by weight and fasting blood glucose and then dosed with either vehicle (2% Tween 80 and 0.5% methyl cellulose) or ertiprotafib at 25 mg/kg/day for 4 days. After treatment, mice treated with ertiprotafib had their fasting glucose levels returned to the normal range in the context of markedly reduced insulin levels. Thus, ertiprotafib seemed to increase insulin sensitivity in these mice after short-term treatment. It is noteworthy that serum triglyceride levels were also markedly reduced in these treated animals (see below).

To further test the ability of ertiprotafib to increase insulin sensitivity, male Zucker *fa/fa* rats were dosed with ertiprotafib or compound 3 at either 25 or 5 mg/kg/day for 14 days. Fasting blood glucose levels were measured, and an oral glucose tolerance test was performed on day 10 of dosing, whereas insulin, triglyceride, and free fatty acid levels were measured at the end of the 14-day dosing. As seen with treatment of *ob/ob* mice, both compounds seemed to significantly improve glucose metabolism in rats (Table 2 and Fig. 2). At 25 mg/kg/day, these compounds decreased both fasting blood glucose and insulin levels compared with vehicle treated rats (Table 2). Furthermore, both ertiprotafib and

TABLE 1
Ertiprotafib lowers glucose, insulin, and triglycerides in *ob/ob* mice

Treatment	Body Weight		Fasting Blood Glucose		Insulin After	Triglycerides After
	Before	After	Before	After		
	g		*mg/dl*		*ng/ml*	*mg/dl*
Vehicle	48.1 ± 0.8	48.0 ± 1.0	101 ± 4	102 ± 10	8.4 ± 0.7	42.7 ± 1.5
Ertiprotafib	48.1 ± 0.8	49.5 ± 0.8	102 ± 4	76 ± 2[a,d]	2.5 ± 0.5[b]	32.9 ± 2.5[c]

[a] $p < 0.05$ compared with vehicle.
[b] $p < 0.001$ compared with vehicle.
[c] $p < 0.01$ compared with vehicle.
[d] $p < 0.0001$ compared with before treatment.

TABLE 2
Ertiprotafib and compound 3 lower glucose, insulin, triglycerides, and free fatty acids in *fa/fa* rats

Rats	Treatment	Dose	Fasting Blood Glucose	Insulin	Triglycerides	Free Fatty Acids
			mg/dl	*ng/ml*	*mg/dl*	*μmol/l*
Lean			68 ± 5	3.7 ± 0.3	118 ± 11	640 ± 50
fa/fa	Vehicle		115 ± 18	15.8 ± 1.8	1060 ± 190	1620 ± 160
fa/fa	Ertiprotafib	25 mg/kg	78 ± 5*	9.8 ± 0.7*	260 ± 30*	560 ± 40*
fa/fa	Ertiprotafib	5 mg/kg	99 ± 4	13.1 ± 1.4	770 ± 230	1160 ± 210
fa/fa	Compound 3	25 mg/kg	77 ± 8*	7.3 ± 0.6*	147 ± 18*	450 ± 40*
fa/fa	Compound 3	5 mg/kg	92 ± 3	13.6 ± 1.1	550 ± 70	870 ± 40*

* $p < 0.05$ compared with vehicle.

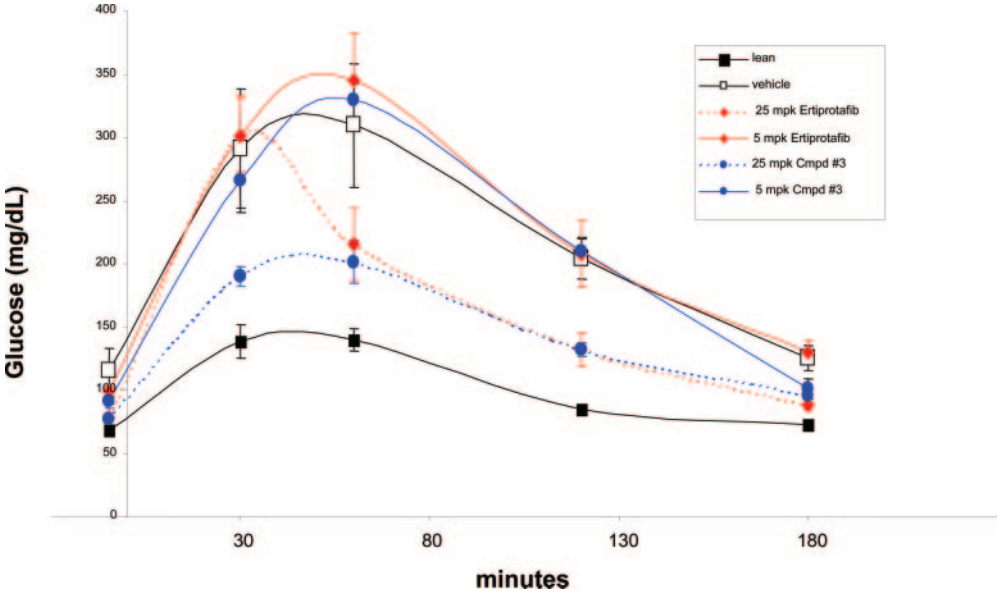

Fig. 2. Ertiprotafib and compound 3 increase glucose disposal in Zucker *fa/fa* rats. Male Zucker *fa/fa* rats were dosed orally for 10 days (see *Materials and Methods*) with vehicle, ertiprotafib, or compound 3 at 25 mg/kg or 5 mg/kg per day as indicated. After a 12-h fast, animals received an oral bolus of glucose (2 g/kg) and blood glucose was measured at the indicated times by tail bleeds.

compound 3 increased glucose disposal after an oral challenge (Fig. 2). Compound 3 seemed to work slightly better at this dose, consistent with its two-fold greater exposure after oral dosing (data not shown), but neither compound was efficacious at the 5 mg/kg/day dose. It is noteworthy that lipid levels were also reduced in treated animals (Table 2). Both triglyceride and free fatty acid levels were substantially reduced in rats treated with 25 mg/kg/day of either compound. Again, compound 3 may be slightly more potent, with free fatty acids levels reduced even at the 5 mg/kg/day dose of this compound. To summarize, both ertiprotafib and compound 3 seem to be robust agents in improving glucose utilization in *fa/fa* rats while also decreasing lipid levels in these animals.

Decreased lipid levels (especially free fatty acids) may be unexpected for a pure PTP1b inhibitor (Klaman et al., 2000). It was more telling, as mentioned above, that rats treated with suprapharmacologic doses of ertiprotafib showed signs of PPAR family activation (peroxisome proliferation, adipose deposition in bone marrow) (Peterson et al., 2004). Because engagement of PPAR family members could contribute to the efficacy seen here, we re-examined the actions of ertiprotafib in vitro to gain a more complete understanding of its mechanism(s) of action.

In this study, we see that ertiprotafib does not behave as a simple, competitive inhibitor of PTP1b. Inhibition follows a time-dependent, irreversible mechanism that displays nonclassic kinetics (Fig. 3a and Table 3). It is very revealing that this inhibition was dependent on the concentration of enzyme used in each assay, a hallmark of complex inhibition (Table 3). In addition, IC_{50} values for this class of compounds in cell-free assays of PTP1b enzymatic activity vary depending on each assay's components and their interactions with these nonpolar compounds (data not shown). For example, adding small amounts of the nonionic detergent, Triton X-100, shifts the inhibition curve with ertiprotafib (Table 3). Similar results have been found for compounds related to this series (Burkey et al., 2002; Johnson et al., 2002). Thus, PTP1b inhibition by ertiprotafib must be understood in the context of compounds with similar, complex behavior (Doman et al., 2002; McGovern et al., 2002).

To define the concentrations required to inhibit PTP1b in the cellular milieu, we first used a simplified cellular assay expressing recombinant PTP1b in the baculovirus system in sf21 insect cells and measuring turnover of pNPP as reported previously (Cromlish et al., 1999). In this assay (Fig. 3b),

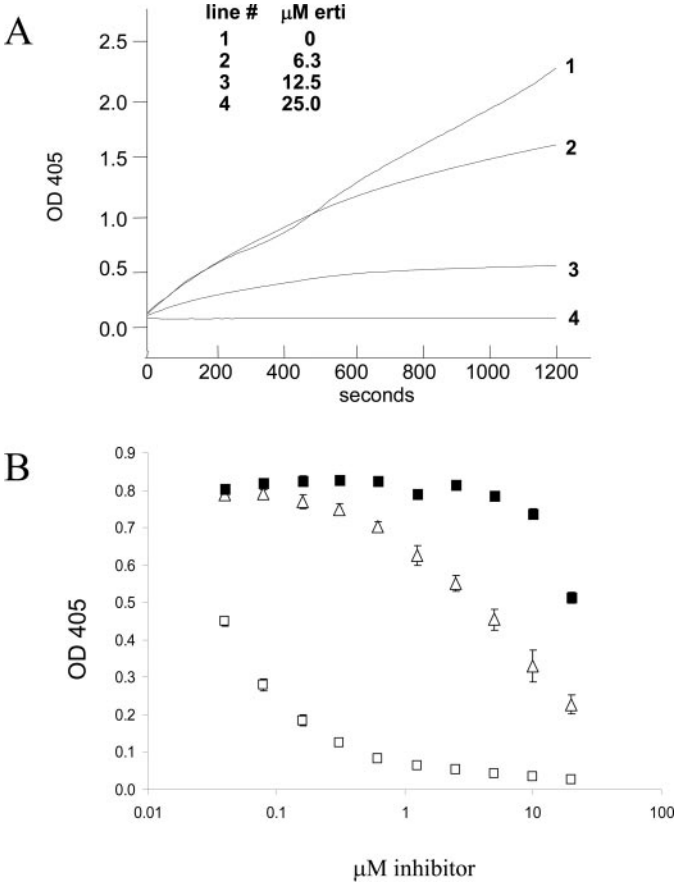

Fig. 3. A, ertiprotafib inhibition is time-dependent. pNPP cleavage by PTP1b was monitored over time in the presence of the indicated concentrations of ertiprotafib as described under *Materials and Methods*. B, inhibition of PTP1b in sf21 cells. PTP1b cleavage of pNPP was measured using sf21 cells (see *Materials and Methods*) after a 30-min preincubation with the indicated concentrations of vanadate (□), compound 33 (△), or ertiprotafib (■).

TABLE 3

Inhibition by ertiprotafib: effects of [E] and detergent

IC_{50} values were determined for inhibition of pNPP turnover as described under *Materials and Methods* at two different enzyme concentrations in the presence or absence of added Triton X-100.

Conc PTP1b	Triton X-100	
	None	0.01%
	μM	
10 nM	1.6	16
100 nM	9	29

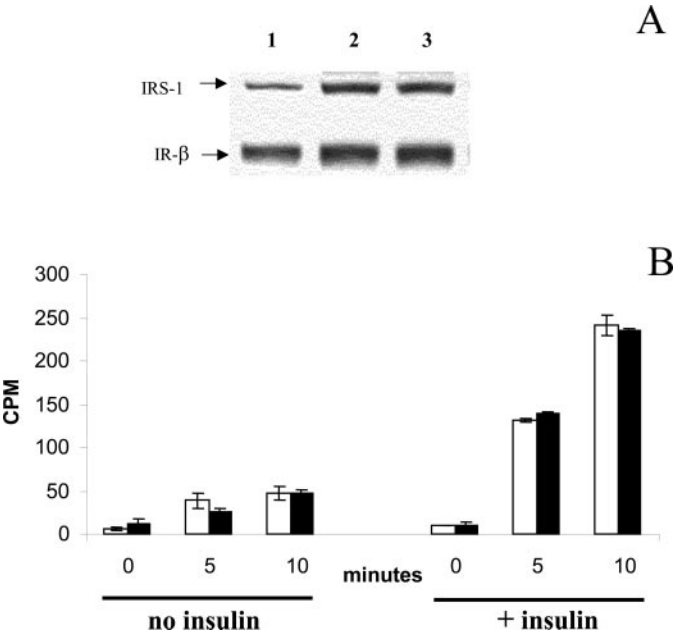

Fig. 4. Effect of ertiprotafib signaling in 3T3-L1 adipocytes. A, IR and IRS-1 dephosphorylation after insulin withdrawal was measured in 3T3-L1 adipocytes treated with DMSO (lane 1), 10 μM vanadate (lane 2), or 10 μM ertiprotafib (lane 3) before blotting with anti-pTyr antibodies (see *Materials and Methods*). Identities of each band were confirmed by stripping and blotting with IR-β and IRS-1–specific antibodies (not shown). B, glucose uptake by 3T3-L1 adipocytes was measured after incubation with or without insulin as indicated either alone (open bars) or with 20 μM ertiprotafib (filled bars) as described under *Materials and Methods*.

both vanadate and the known, reversible PTP1b inhibitor compound 33 (see Fig. 1 for structure from Taing et al., 1999) give inhibition constants of 0.1 and 4.5 μM, respectively, consistent with literature values (Huyer et al., 1997; Cromlish et al., 1999; Taing et al., 1999). Ertiprotafib, on the other hand, inhibits with an IC_{50} greater than 20 μM (Fig. 3b). Similar results were found for compound 3, with an IC_{50} greater than 20 μM (not shown). As in cell-free assays, inhibition by ertiprotafib (but not the control compounds vanadate and compound 33) in this cellular assay varied with assay components and with time, with greater inhibition seen at lower enzyme levels and later time points (data not shown).

Next, potential effects of ertiprotafib on PTP1b regulation of insulin signaling were investigated in 3T3-L1 cells differentiated into adipocytes by standard procedures (Frost and Lane, 1985). Cells were preincubated with inhibitor for 30 min, pulsed with insulin for 10 min, washed, and compounds were added back for another hour before harvest, lysis, electrophoresis and blotting with anti-phosphotyrosine antibodies. This time after insulin withdrawal allows measurement of the rate of dephosphorylation of the insulin receptor and proximal signaling molecules in the presence of inhibitors. Although no significant difference in phosphorylation of the insulin receptor was seen with either vanadate or ertiprotafib, both treatments did give about a 2-fold increase in tyrosine phosphorylation of the downstream molecule IRS-1 (Fig. 4a). The short incubation period makes it likely that this effect occurs through phosphatase inhibition, presumably PTP1b, although at these concentrations, effects on other phosphatases cannot be ruled out. This increase in IRS-1 phosphorylation did not translate into increased glucose uptake by these cells, however. As seen in Fig. 4b, no increase in glucose uptake by the differentiated 3T3-L1 cells

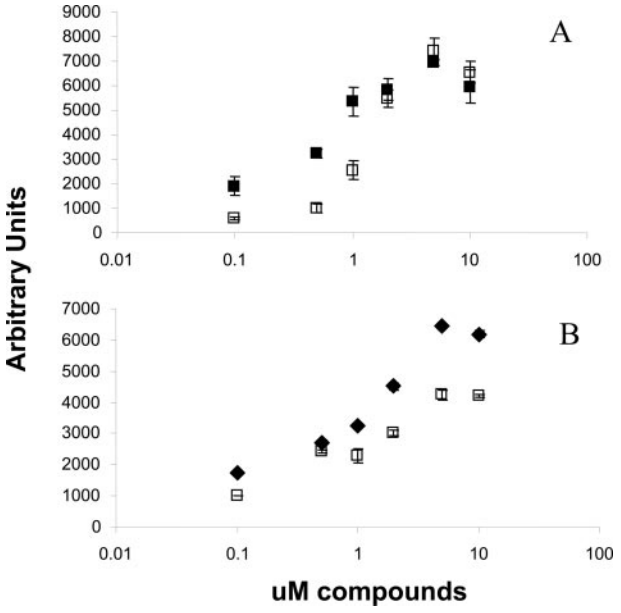

Fig. 5. Ertiprotafib activates transcription through PPARα and PPARγ. A, CV-1 cells were transfected with the luciferase reporter construct (pGL-3-PPRE) and a PPARα expression construct (pED.PPARα) before treatment with ciprofibrate (■) or ertiprotafib (□) and measurement of induced luciferase activity as described under *Materials and Methods*. B, CV-1 cells were transfected with the luciferase reporter construct (pGL-3-PPRE) and a PPARγ expression construct (pED.PPARγ) before treatment with troglitazone (♦) or ertiprotafib (□) and measurement of induced luciferase activity as described under *Materials and Methods*. Luciferase activity is expressed in arbitrary units after subtraction of background luminescence resulting from cells transfected with empty plasmids.

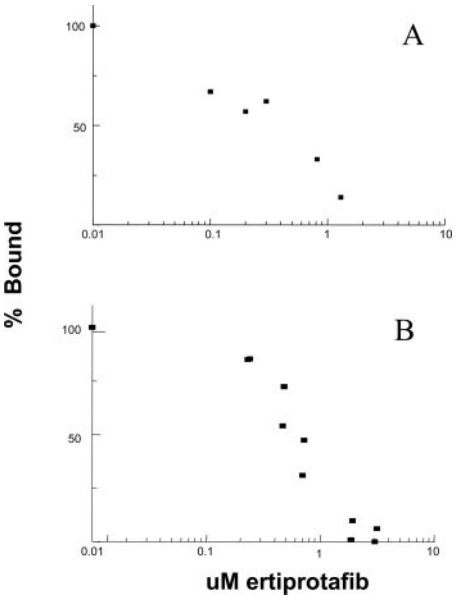

Fig. 6. Ertiprotafib competes for binding of fatty acids to PPARα and PPARγ. A, the recombinant PPARα ligand binding domain was expressed in *E. coli* as a poly-histidine–tagged fusion and purified by nickel affinity chromatography for use in a competitive displacement assay with the fluorescent fatty acid 12-anthracene oleic acid as described previously (Palmer and Wolf, 1998; Causevic et al., 1999). Results are expressed as the percentage of 12-anthracene oleic acid bound (after subtraction of background fluorescence from protein or fatty acid alone) in the presence of the indicated concentrations of ertiprotafib, compared with binding in the absence of ertiprotafib. B, ertiprotafib was assayed for its ability to bind PPARγ as in A, but with *cis*-parinaric acid as the reporter ligand, again as described previously (Palmer and Wolf, 1998; Causevic et al., 1999).

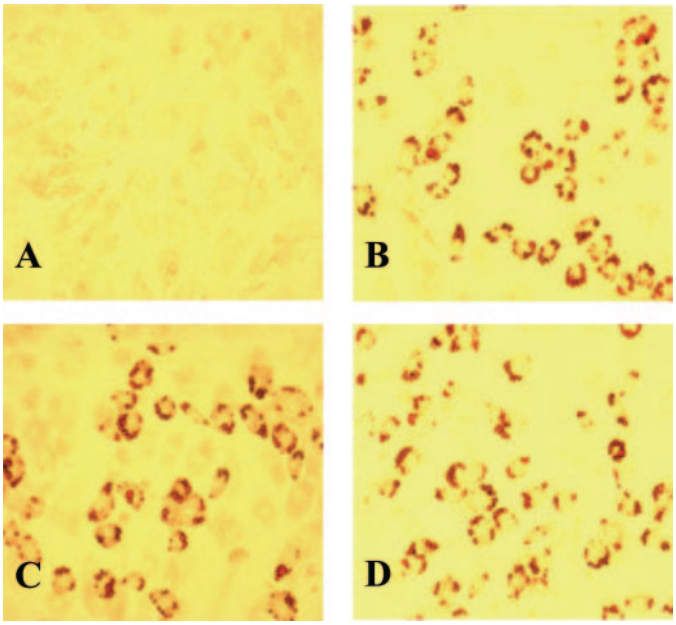

Fig. 7. Ertiprotafib and its analog induce adipocyte differentiation. C3H10T1/2 cells were differentiated into adipocytes (see *Materials and Methods*) in the presence of either DMSO (A), 50 nM rosiglitazone (B), 10 μM ertiprotafib (C), or 10 μM compound 3 (D) before staining with Oil Red O to visualize fat droplets.

was seen with ertiprotafib either alone or with insulin. Similar results were seen with cultured myocytes (data not shown). Taken together, these assays of phosphatase inhibition and insulin signaling indicate that although ertiprotafib inhibits PTP1b in cells, this inhibition occurs at relatively high concentrations (under the specified assay conditions) and may not provide a full explanation of its in vivo efficacy.

To evaluate whether agonism of PPAR family members might play a role in the pharmacology of ertiprotafib, a reporter system was employed using luciferase as the readout. Three copies of the DNA for the consensus PPAR response element (PPRE) were inserted upstream of the SV40 promoter and luciferase gene (reporter plasmid pGL3). This was cotransfected into CV-1 cells along with expression plasmids for either PPARα or PPARγ. Test compounds were then added at various concentrations for 40 h (to allow expression of each PPAR and induced transcription of luciferase) before cell lysis and quantification of luciferase activity. As seen in Fig. 5, ertiprotafib seems to activate transcription through both PPARα and PPARγ at concentrations similar to known agonists. Here, ciprofibrate gave dose-dependent stimulation of PPARα driven transcription of luciferase (EC_{50} of 0.6 $\pm$ 0.2 μM). Ertiprotafib also seemed to drive PPARα-dependent transcription to the same extent, with an EC_{50} of 1.4 $\pm$ 0.5 μM. In Fig. 5b, one sees that ertiprotafib also activates transcription through PPARγ (EC_{50} of 1.1 $\pm$ 0.4 μM), although the magnitude of the response was less than the known PPARγ agonist troglitazone (EC_{50} of 1.7 $\pm$ 0.1 μM), indicating partial agonism of this receptor by ertiprotafib. Ertiprotafib activation of each PPAR seems to be direct. Figure 6 shows the results of experiments using ertiprotafib to compete for binding of fluorescent fatty acids to each PPAR. In this study, we see competitive displacement of fatty acid binding to PPARα with an IC_{50} of 0.5 μM (Fig. 6a) and displacement of fatty acid binding to PPARγ with an IC_{50} of 0.6 μM (Fig. 6b).

The transactivation of PPARγ by ertiprotafib also results in relevant responses in cells, as measured by adipocyte differentiation of the murine fibroblast line C3H/10T 1/2 (Fig. 7). This assay was used in identification of PPAR ligands and has been clearly shown to reflect induction of the adipocyte phenotype in a PPARγ-dependent manner (Forman et al., 1995). In these assays, fibroblasts are treated with compounds and insulin for a total of 4 to 6 days, washed, fixed, and stained with oil red to visualize the fat droplets that form as a result of adipogenesis. In Fig. 7, one sees the comparison between control cells treated with DMSO alone (A) and cells treated with the known PPARγ agonist rosiglitazone (B), or the test compounds ertiprotafib (C) and compound 3 (D). One can clearly see the increase in cells staining positive for fat droplets with oil red when treated with rosiglitazone (Fig. 7B). Ertiprotafib and compound 3 were evaluated in these same cells and also seemed to drive adipogenesis (Fig. 7, C and D). Therefore, not only does ertiprotafib transactivate PPARγ in the reporter gene systems, it also serves as bona fide inducer of adipogenesis in fibroblast cells. In fact, compared with rosiglitazone, a known PPARγ agonist, both ertiprotafib and its analog improve glycemic excursion to a sim-

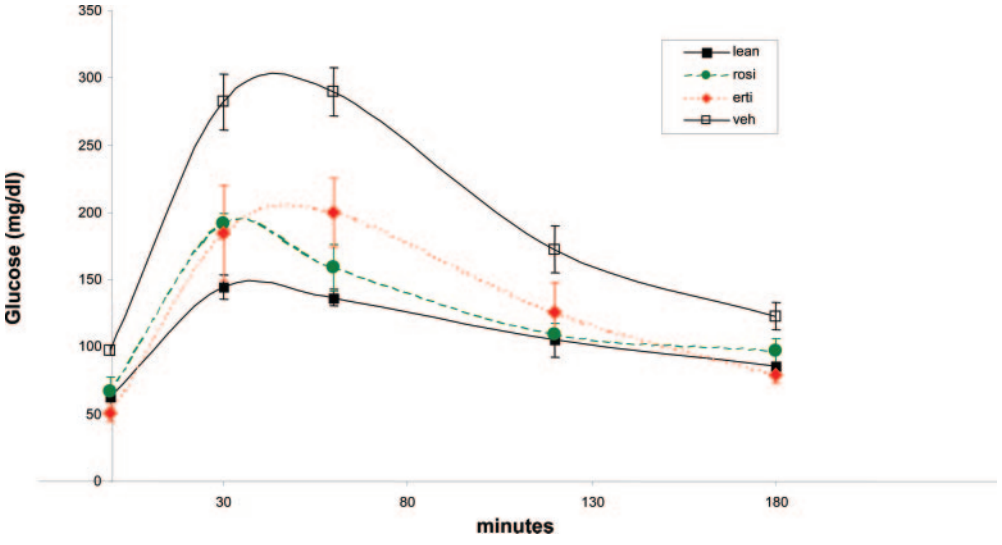

Fig. 8. Ertiprotafib and rosiglitazone increase glucose disposal to comparable levels. Male Zucker *fa/fa* rats were dosed for 14 days with either vehicle (2% Tween 80, 0.5% methyl cellulose), 3 mg/kg rosiglitazone, or 25 mg/kg ertiprotafib as described under *Materials and Methods*. After a 12-h fast, treated animals (as well as untreated lean control rats) received an oral bolus of glucose (2 g/kg) before measurement of blood glucose levels by tail bleeds (see *Materials and Methods*).

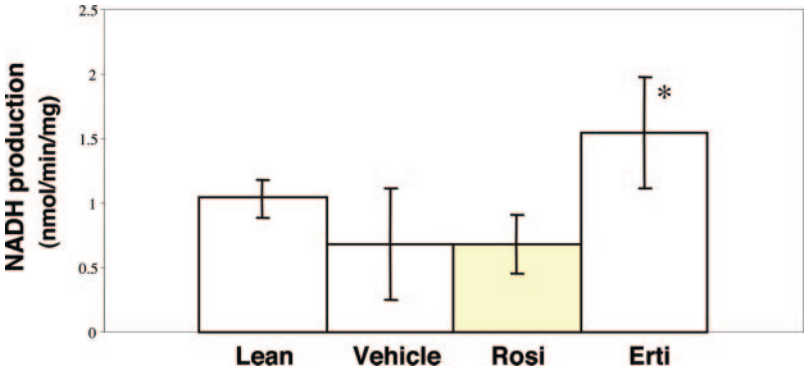

Fig. 9. Ertiprotafib induces fatty acid oxidation in the livers of treated animals. Livers from the Zucker lean and *fa/fa* rats (see Fig. 7) treated 14 days of dosing with either 3 mg/kg rosiglitazone, 25 mg/kg ertiprotafib, or vehicle were assayed for NADH production as described under *Materials and Methods*. For each group, $n = 4$. *, $P < 0.005$ by analysis of variance compared with vehicle-treated animals.

ilar extent after an oral glucose tolerance test in *fa/fa* rats (Fig. 8).

Last, one sees evidence for the relevance of PPARα engagement in vivo by ertiprotafib, through induction of a PPARα-responsive enzyme in treated animals (Fig. 9). In this study, CN^--insensitive palmitoyl-CoA oxidase activity was measured in the isolated microsomes of liver from animals treated with either ertiprotafib or rosiglitazone versus vehicle-treated and lean control rats. One sees no difference in activity in *fa/fa* rats treated with either vehicle or rosiglitazone (even compared with lean control rats). Ertiprotafib treatment, however, significantly increased oxidase activity (Fig. 9). Thus, one sees evidence of PPARα engagement by ertiprotafib under conditions in which efficacy is seen.

Discussion

Ertiprotafib was initially targeted as a PTP1b inhibitor for the treatment of type 2 diabetes and progressed as far as phase II clinical trials before its development was discontinued. The present study sought to clarify its mechanism(s) of action to aid in interpretation of these results. In this study, PTP1b inhibition by ertiprotafib was shown to follow nonclassic kinetics; results were dependent on the time of incubation as well as assay components such as enzyme concentration. A common mechanism has recently been described for many of the poorly behaved inhibitors that result from screening efforts (Doman et al., 2002; McGovern et al., 2002). Compounds of this type form higher order aggregates that have been visualized by electron microscopy. Their inhibitory properties are dependent upon this aggregation, resulting in nonclassic kinetics. Two signatures of such inhibition are changes in IC_{50} values with either a change in enzyme concentration or addition of a small amount of detergent (McGovern et al., 2002; B. Shoichet, unpublished observations). Both phenomena were seen in the characterization of ertiprotafib. This demonstration of poorly behaved kinetics confounds estimates of potency versus PTP1b in vivo. Ertiprotafib did seem here to inhibit PTP1b in cellular assays (including delaying de-phosphorylation of IRS-1 in adipocytes) albeit at relatively high concentrations. Ertiprotafib treatment of either fat or muscle cells did not translate into a short term increase in glucose uptake, although these assays may not be sensitive enough to see a partial effect of PTP1b inhibition. Thus, these data indicated that although PTP1b inhibition probably plays some role in the pharmacology of ertiprotafib, potent inhibition of PTP1b seems an unlikely explanation for its complete pharmacological profile.

The data presented here indicate that (in addition to inhibiting PTP1b) ertiprotafib is at least a dual PPARα and PPARγ agonist with EC_{50} values for transactivation of ~1 μM. Such activities readily explain the observations with suprapharmacologic doses of these compounds (see above) while also contributing to the pharmacology seen at efficacious doses. The efficacy results presented show that ertiprotafib and its analog, compound 3, lowered plasma glucose levels, reduced insulinemia, lowered serum triglycerides, and lowered free fatty acid levels in rodent models of type 2 diabetes. It is noteworthy that similar results were seen when these same animal models were used in the evaluation of thiazolidinediones (Spiegelman, 1998). Although a PTP1b inhibitor could be expected to decrease glucose, insulin, and triglyceride levels based upon the phenotype of the knockout mice, free fatty acid levels were not different in these animals (Klaman et al., 2000). PPARα ligands, however, are able to lower both serum triglycerides and free fatty acids in rodents (Staels et al., 1998; Chou et al., 2002) and are able to improve insulin sensitivity (Guerre-Millo et al., 2000). Thus, given the increase in acyl-CoA oxidase activity in the livers of treated animals, it seems likely that PPARα agonism (in addition to PPARγ agonism and PTP1b inhibition) may contribute to the drop in fatty acid levels seen with ertiprotafib treatment, along with a portion of the glucose and insulin lowering. In fact, the livers of Sprague-Dawley rats treated with ertiprotafib showed widespread up-regulation of genes involved in lipid metabolism, peroxisome proliferation, and fatty acid β-oxidation (Peterson et al., 2004). These animals also exhibited increased liver weights and hepatocellular hypertrophy, along with decreased cholesterol and triglyceride levels. Furthermore, many of the genes with increased liver expression after ertiprotafib treatment are known to be PPARα-regulated, including acyl-CoA oxidase, PEX11α, and CYP4A1 (Peterson et al., 2004). These animals also showed induction of the PPARγ-regulated gene CD36 in ovaries as well as multiple PPARγ-dependent genes in fat (R. Peterson, R. Jordan, A. Dorner, unpublished observations). Although these studies were performed at doses of ertiprotafib higher than those needed for efficacy, the results are consistent with the data presented here and indicate that PPAR agonism probably contributes to the pharmacology seen with ertiprotafib. In fact, preliminary experiments indicate that ertiprotafib is able to transactivate gene expression through PPARδ as well, with an EC_{50} of 5 μM (C. R. Elcombe, unpublished observations). Because agonism of PPARδ can be expected to mediate effects in vivo similar to those shown here (Wang et al., 2003), this nuclear receptor may also contribute to the pharmacology observed with ertiprotafib. What portion each of the targets discussed here (PTP1b, PPARα, PPARγ, PPARδ) may play in the pharmacology of ertiprotafib, as well as potential contributions from other targets (e.g., RXR), requires further study.

In conclusion, results from both in vitro and in vivo experiments indicate that the improvements in peripheral insulin sensitivity (normalizing plasma glucose while reducing insulin levels) and reductions in hyperlipidemia after treatment with ertiprotafib are probably caused by a combination of mechanisms. These data should inform interpretations from results of clinical trials with ertiprotafib and aid in the search for improved insulin sensitizers.

Acknowledgments

We thank Dr. Zhong-Yin Zhang for compound 33, Drs. Arlene Dietrich, Madelene Antane, Paul Dollings, and Jay Wrobel for ertiprotafib and compound 3, Dr. Clifford Elcombe for fatty acid binding studies, and Richard Maylor for helpful advice and discussion.

References

Aitio A and Vainio H (1976) UDP glucuronosyltransferase and mixed function oxidase activity in microsomes prepared by differential centrifugation and calcium aggregation. *Acta Pharmacol Toxicol* **39:**555–561.

Brooks DA, Etgen GJ, Rito CJ, Shuker AJ, Dominianni SJ, Warshawsky AM, Ardecky R, Paterniti JR, Tyhonas J, Karanewsky DS, et al. (2001) Design and synthesis of 2-methyl-2-{4-[2-(5-methyl-2-aryloxazol-4-yl)ethoxy]phenoxy}propionic acids: a new class of dual PPARα/γ agonists. *J Med Chem* **44:**2061–2064.

Burkey BF, Dong M, Wennogle L, Babb R, Dressman M, Islam A, Deacon R, Dragland C, Kaplan E, Tomesch J, et al. (2002) Pharmacogenomic evaluation of a putative orally active PTP-1B inhibitor using *ob/ob* mice reveals an alternative mechanism of action. *Diabetes* **51 Suppl:** abstract 138.
Causevic M, Wolf CR, and Palmer CNA (1999) Substitution of a conserved amino acid residue alters the ligand binding properties of peroxisome proliferator activated receptors. *FEBS Lett* **463:**205–210.
Cheng A, Uetani N, Simoncic PD, Chaubey VP, Lee-Loy A, McGlade CJ, Kennedy BP, and Tremblay ML (2002) Attenuation of leptin action and regulation of obesity by protein tyrosine phosphatase 1B. *Dev Cell* **2:**385–387.
Chou CJ, Haluzik M, Gregory C, Dietz KR, Vinson C, Gavrilova O, Reitman ML (2002) WY14,643, a peroxisome proliferator-activated receptor α (PPARα) agonist, improves hepatic and muscle steatosis and reverses insulin resistance in lipoatrophic A-ZIP/F-1 mice. *J Biol Chem* **277:**24484–24489.
Cromlish WA, Payette P, and Kennedy BP (1999) Development and validation of an intact cell assay for protein tyrosine phosphatases using recombinant baculoviruses. *Biochem Pharm* **58:**1539–1546.
Cronet P, Petersen JF, Folmer R, Blomberg N, Sjoblom K, Karlsson U, Lindstedt EL, and Bamberg K (2001) Structure of the PPAR-alpha and -gamma ligand binding domain in complex with AZ 242; ligand selectivity and agonist activation in the PPAR family. *Structure (Camb.)* **9:**699–706.
Diamant M and Heine RJ (2003) Thiazolidinediones in type 2 diabetes mellitus: current clinical evidence. *Drugs* **63:**1373–1405.
Doman TN, McGovern SL, Witherbee BJ, Kasten TP, Kurumbail R, Stallings WC, Connolly DT, and Shoichet BK (2002) Molecular docking and high-throughput screening for novel inhibitors of protein tyrosine phosphatase-1B. *J Med Chem* **45:**2213–2221.
Elchebly M, Payette P, Michaliszyn E, Cromlish W, Collins S, Loy AL, Normandin D, Cheng A, Himms-Hagen J, Chan C-C, et al. (1999) Increased insulin sensitivity and obesity resistance in mice lacking the protein tyrosine phosphatase-1b gene. *Science (Wash DC)* **283:**1544–1548.
Flier JS (2004) Obesity wars: molecular progress confronts an expanding epidemic. *Cell* **116:**337–350.
Forman BM, Tontonoz P, Chen J, Brun RP, Spiegelman BM, and Evans RM (1995) 15-deoxy-$\Delta^{12,14}$-prostaglandin J_2 is a ligand for the adipocyte determination factor PPARγ cell **83:**803–812.
Frost SC and Lane MD (1985) Evidence for the involvement of vicinal sulfhydryl groups in insulin-activated hexose transport by 3T3–L1 adipocytes. *J Biol Chem* **260:**2646–2652.
Gray TJB, Lake BG, Beamand JA, Foster JR, and Gangolli SD (1983) Peroxisome proliferation in primary cultures of rat hepatocytes. *Toxicol Appl Pharmacol* **67:**15–25.
Guerre-Millo M, Gervois P, Raspe E, Madsen L, Poulain P, Derudas B, Herbert J-M, Winegar DA, Willson TM, Fruchart J-C, et al. (2000) Peroxisome proliferator-activated receptor α activators improve insulin sensitivity and reduce adiposity. *J Biol Chem* **275:**16638–16642.
Gum RJ, Gaede LL, Koterski SL, Heindel M, Clampit JE, Zinker BA, Trevillyan JM, Ulrich RG, Jirousek MR, and Rondinone CM (2003) Reduction of protein tyrosine phosphatase 1B increases insulin-dependent signaling in *ob/ob* mice. *Diabetes* **52:**21–28.
Huyer G, Liu S, Kelly J, Moffat J, Payette P, Kennedy B, Tsaprailis G, Gresser MJ, and Ramachandran C (1997) Mechanism of inhibition of protein-tyrosine phosphatases by vanadate and pervanadate. *J Biol Chem* **272:**843–851.
Inzucchi SE (2002) Oral antihyperglycemic therapy for type 2 diabetes: scientific review. *J Am Med Assoc* **287:**360–372.
Johnson TO, Ermolieff J, and Jirousek MR (2002) Protein tyrosine phosphatase 1B inhibitors for diabetes. *Nat Rev Drug Disc* **1:**696–709.
Kaufman RJ, Davies MV, Wasley LC, and Michnick D (1991) Improved vectors for stable expression of foreign genes in mammalian cells by use of the untranslated leader sequence from EMC virus. *Nucleic Acids Res* **19:**4485–4490.
Kersten S, Desvergne B, and Wahli W (2000) Roles of PPARs in health and disease. *Nature (Lond)* **405:**421–424.
Klaman LD, Boss O, Peroni OD, Kim JK, Martino JL, Zabolotny JM, Moghal N, Lubkin M, Kim Y-B, Sharpe AH, et al. (2000) Increased energy expenditure, decreased adiposity, and tissue-specific insulin sensitivity in protein-tyrosine phosphatase 1b-deficient mice. *Mol Cell Biol* **20:**5479–5489.
Liu KG, Smith JS, Ayscue AH, Henke BR, Lambert MH, Leesnitzer LM, Plunket KD, Willson TM, Sternbach DD (2001) Identification of a series of oxadiazole-substituted alpha-isopropoxy phenylpropanoic acids with activity on PPARalpha, PPARgamma and PPARdelta. *Bioorg Med Chem Lett* **11:**2385–2388.
Lohray BB, Lohray VB, Bajji AC, Kalchar S, Poondra RR, Padakanti S, Chakrabarti R, Vikramadithyan RK, Misra P, Juluri S, et al. (2001) (−)3-[4-[2-(phenoxazin-10-yl)ethoxy]phenyl]-2-ethoxypropanoic acid [(−) DRF 2725]: a dual PPAR agonist with potent antihyperglycemic and lipid modulating activity. *J Med Chem* **44:**2675–2678.
McGovern SL, Caselli E, Grigorieff N, and Shoichet BK (2002) A common mechanism underlying promiscuous inhibitors from virtual and high-throughput screening. *J Med Chem* **45:**1712–1722.
Murakami K, Tobe K, Ide T, Mochizuki T, Ohashi M, Akanuma Y, Yazaki Y, and Kadowaki T (1998) A novel insulin sensitizer acts as a coligand for peroxisome proliferator-activated receptor-α (PPAR-α) and PPAR-γ: effect of PPARα activation on abnormal lipid metabolism in liver of Zucker fatty rats. *Diabetes* **47:**1841–1847.
Nesto RW, Bell D, Bonow RO, Fonseca V, Grundy SM, Horton ES, Winter ML, Porte D, Semenkovich CF, Smith S, et al. (2003) Thiazolidinedione use, fluid retention and congested heart failure. *Circulation* **108:**2941–2948.
Palmer CNA and Wolf CR (1998) *cis*-Parinic acid is a ligand for the human peroxisome proliferator activated receptor γ: development of a novel spectrophotometric assay for the discovery of PPARγ ligands. *FEBS Lett* **431:**476–480.
Peterson RL, Casciotti L, Block L, Goad MEP, Tong Z, Meehan JT, Jordan RA, Vinlove MP, Markiewicz VR, Weed CA, et al. (2004) Mechanistic toxicogenomic analysis of WAY-144112 (ertiprotafib) administration in Sprague-Dawley rats. *Toxicol Appl Pharmacol* **196:**80–94.
Rosen ED and Spiegelman BM (2001) PPARγ: a nuclear regulator of metabolism, differentiation and cell growth. *J Biol Chem* **276:**37731–37734.
Spiegelman BM (1998) PPAR-γ: adipogenic regulator and thiazolidinedione receptor. *Diabetes* **47:**507–514.
Staels B, Dallongeville J, Auwerx J, Schoonjans K, Leitersdorf E, and Fruchart JC (1998) Mechanism of action of fibrates on lipid and lipoprotein metabolism. *Circulation* **98:**2088–2093.
Taing M, Keng Y-F, Shen K, Wu L, Lawrence DS, and Zhang Z-Y (1999) Potent and highly selective inhibitors of the protein tyrosine phosphatase 1B. *Biochemistry* **38:**3793–3803.
Wang Y-X, Lee C-H, Tiep S, Yu RT, Ham J, Kang H, and Evans RM (2003) Peroxisome-proliferator-activated receptor δ activates fat metabolism to prevent obesity. *Cell* **113:**159–170.
Way JM, Harrington WW, Brown KK, Gottschalk WK, Sundseth SS, Mansfield TA, Ramachandran RK, Willson TM, and Kliewer SA (2001) Comprehensive messenger ribonucleic acid profiling reveals that peroxisome proliferator-activated receptor gamma activation has coordinate effects on gene expression in multiple insulin-sensitive tissues. *Endocrin* **142:**1269–1277.
Willson TM, Brown PJ, Sternbach DD, and Henke BR (2000) The PPARs: from orphan receptors to drug discovery. *J Med Chem* **43:**527–550.
Willson TM, Lambert MH, and Kliewer SA (2001) Peroxisome proliferator-activated receptor g and metabolic disease. *Annu Rev Biochem* **70:**341–367.
Wrobel J, Sredy J, Moxham C, Dietrich A, Li Z, Sawicki DR, Seestaller L, Wu L, Katz A, Sullivan D, et al. (1999) PTP1b inhibition and antihyperglycemic activity in the *ob/ob* mouse model of novel 11-arylbenzo[b]naphtho[2,3-d]furans and 11-arylbenzo[b]naphtho[2,3-d]thiophenes. *J Med Chem* **42:**3199–3202.
Zabolotny JM, Bence-Hanulec KK, Stricker-Krongrad A, Haj F, Wang Y, Minokoshi Y, Kim YB, Elmquist JK, Tartaglia LA, Kahn BB et al. (2002) PTP1B regulates leptin signal transduction *in vivo*. *Dev Cell* **2:**489–495.
Zinker BA, Rondinone CM, Trevillyan JM, Gum RJ, Clampit JE, Waring JF, Xie N, Wilcox D, Jacobson P, Frost L, et al. (2002) PTP1B antisense oligonucleotide lowers PTP1B protein, normalizes blood glucose and improves insulin sensitivity in diabetic mice. *Proc Natl Acad Sci USA* **99:**11357–11362.

Address correspondence to: David V. Erbe, Wyeth Research, Cardiovascular and Metabolic Diseases, 200 Cambridge Park Drive, Cambridge MA 02140. E-mail: derbe@wyeth.com